

## N O T I C E

THIS DOCUMENT HAS BEEN REPRODUCED FROM  
MICROFICHE. ALTHOUGH IT IS RECOGNIZED THAT  
CERTAIN PORTIONS ARE ILLEGIBLE, IT IS BEING RELEASED  
IN THE INTEREST OF MAKING AVAILABLE AS MUCH  
INFORMATION AS POSSIBLE



# Technical Memorandum 80330

## Performance Analysis of the Spaceborne Laser Ranging System

W. D. Kahn, F. O. Vonbun, D. E. Smith,  
T. S. Englar and B. P. Gibbs

(NASA-TM-80330) PERFORMANCE ANALYSIS OF THE  
SPACEBORNE LASER RANGING SYSTEM (NASA) 26 p  
HC A03/MF A01 CSCL 20E

N80-17443

Unclas

G3/36 12901

**OCTOBER 1979**

National Aeronautics and  
Space Administration

**Goddard Space Flight Center**  
Greenbelt, Maryland 20771



**PERFORMANCE ANALYSIS  
OF THE  
SPACEBORNE LASER RANGING SYSTEM**

**W. D. Kahn  
F. O. Vonbun  
D. E. Smith  
GSFC Greenbelt, MD 20771**

**T. S. Englar  
B. P. Gibbs  
Business and Technological Systems, Inc.  
Seabrook, MD 20801**

**GODDARD SPACE FLIGHT CENTER  
Greenbelt, Maryland 20771**

PERFORMANCE ANALYSIS  
OF THE  
SPACEBORNE LASER RANGING SYSTEM

W. D. Kahn  
F. O. Vonbun  
D. E. Smith  
GSFC Greenbelt, MD 20771

T. S. Englar  
B. P. Gibbs  
Business and Technological Systems, Inc.  
Seabrook, MD 20801

ABSTRACT

The Spaceborne Laser Ranging System is a proposed short pulse laser on board an orbiting spacecraft (1, 2, 3, 4). It measures the distances between the spacecraft and many laser retroreflectors (targets) deployed on the earth's surface. The precision of these range measurements is assumed to be about  $\pm 2$  cm (5). These measurements are then used together with the orbital dynamics of the spacecraft, to derive the intersite vector between the laser ground targets. The errors associated with this vector are on the order of 1 to 2 cm. The baseline distances to be determined range from 25 km to 1200 km. By repeating the measurements of the intersite vector, strain and strain rate errors are estimated. These quantities are essential for crustal dynamic studies which include determination and monitoring of strain near seismic zones, land subsidence, and edifice building preceding volcanic eruptions. The realizable precision for intersite distance determination is estimated to be on the order of 0.5 cm at 300 km and about 1.5 cm at 1200 km. The corresponding inaccuracies for the intersite distances are larger, that is 1 cm and 3.5 cm respectively. The corresponding precision in the vertical direction is 1 cm and 3 cm. The accuracies in the vertical direction which can be achieved are 3 cm and 10 cm. These values were obtained for a six day observing period with 50% cloud cover.

It is evident that such a system can also be used for geodetic surveys where such accuracies are generally not needed.

## CONTENTS

	<u>Page</u>
INTRODUCTION .....	1
SYSTEM DESCRIPTION .....	1
INTERSITE DISTANCE ESTIMATION-ANALYSIS .....	3
SIMULATION RESULTS .....	12
CONCLUSION .....	19
ACKNOWLEDGMENTS .....	19
REFERENCES .....	20

PRECEDING PAGE BLANK NOT FILMED

# PERFORMANCE ANALYSIS OF THE SPACEBORNE LASER RANGING SYSTEM

## I. INTRODUCTION

The result of computer simulations demonstrating the precision in determining intersite distances using a spaceborne Laser Ranging System are described. Repeated determinations of intersite distance generate estimates of crustal strain and strain rate. The study of strain and the variation of strain with time are essential parameters for earthquake research (6, 7). It will be shown below that measurement periods of only a few days can yield very high precision measurements which, because of their accuracy and the speed with which they are obtained, can provide a new dimension to earthquake study.

## II. SYSTEM DESCRIPTION

The Spaceborne Laser Ranging System consists of an orbiting spacecraft carrying a pulsed laser distance measurement system that sequentially measures the distance to a number of retroreflector arrays on the ground. Figure 1 shows the general concept of the system. The spacecraft ranges to corner retroreflectors on the Earth's surface as it passes overhead. The proposed laser system consists of a Nd YAG Laser with a 200 picosecond pulse length and a repetition rate of 10 pulses/sec. The RMS range uncertainty of a single pulse at 5 to 10 photo electrons is expected to be 1 to 2 cm with a bias of a few millimeters (8). The ground target (9) will consist of a small corner cube array of retroreflectors mounted on a pillar.

As the first reflector of a ground network comes into view of the spacecraft, an acquisition procedure is initiated that is expected to take 10 to 15 seconds. The procedure consists of a search for the reflector based on a priori knowledge of the reflector's location and the position of the spacecraft. After the acquisition of the first retroreflector, the laser makes 20 to 30 range measurements in a 2 to 3 second period and then swings on to the next reflector, taking less than 0.5 seconds for this operation even for the most widely separated reflectors. The laser dwells 2 to 3 seconds on the second reflector making range measurements and then moves on to the next. No acquisition time is expected to be necessary for the second and subsequent reflectors because

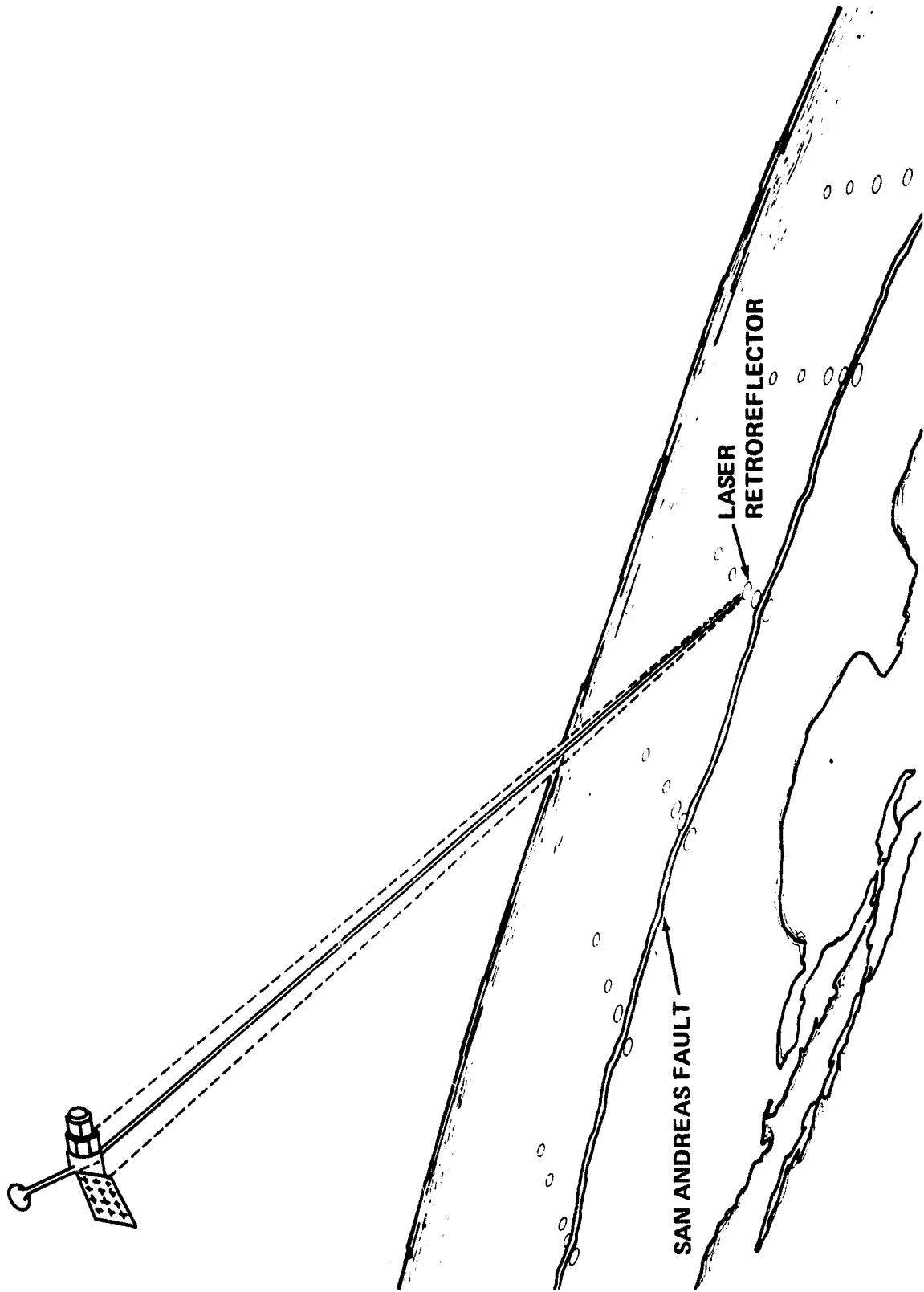


Figure 1. Spaceborne Laser Ranging System

the relative location of the spacecraft and ground network will be updated with the corrected a priori positions obtained during the acquisition of the first reflector.

On any particular pass of the spacecraft over the ground targets, the spaceborne laser will range in a preprogramed fashion to a given reflector approximately three times, each for a 2 to 3 second period; once at a low to medium elevation on approach, once at a high elevation, and once at a medium to low elevation on the way out. For a 1000 km altitude orbit, a pass of the satellite over the target area will last about 10 minutes which implies that about 60 reflector arrays could be surveyed on every pass over the region. The lowest elevation at which measurements are to be made is about 20 degrees to minimize atmospheric refraction. Fig. 2 shows the sequence of events as the spaceborne laser passes over a network.

### III. INTERSITE DISTANCE ESTIMATION-ANALYSIS

In what is to follow, all vectors are referenced to a common geocentric Earth fixed cartesian coordinate system. Furthermore, it is assumed that relatively small effects such as polar motion, Earth and ocean tides are properly modelled.  $S$  represents the vector position of a laser retroreflector (laser target). Suppose that laser range measurements are obtained from  $m$  satellite passes, where  $X_i$ ,  $i = 1, 2, \dots, m$ , is a six-dimensional epoch state for the  $i^{\text{th}}$  pass. The position of the satellite during the  $i^{\text{th}}$  pass at time  $\tau$  can be expressed as

$$U_i(\tau) = U(X_i, \tau) \quad (1)$$

Where the function  $U$  is obtained by integrating the equations of motion with initial conditions provided by  $X_i$  from epoch time  $\tau$ . The measurement of the "round-trip" travel time of a pulse sent from the satellite to the laser target on the ground at time  $\tau$  when scaled by the speed of light is essentially a range measurement. Hence the fundamental measurement is considered to be the range (see Fig. 3), that is:

$$r_i(\tau) = \left[ U_i^T(\tau) U_i(\tau) + S^T S - 2S^T U_i(\tau) \right]^{1/2} \quad (2)$$

Where the observation  $r_i$  is obtained during the  $i^{\text{th}}$  pass.

SPACEBORNE RANGING SYSTEM

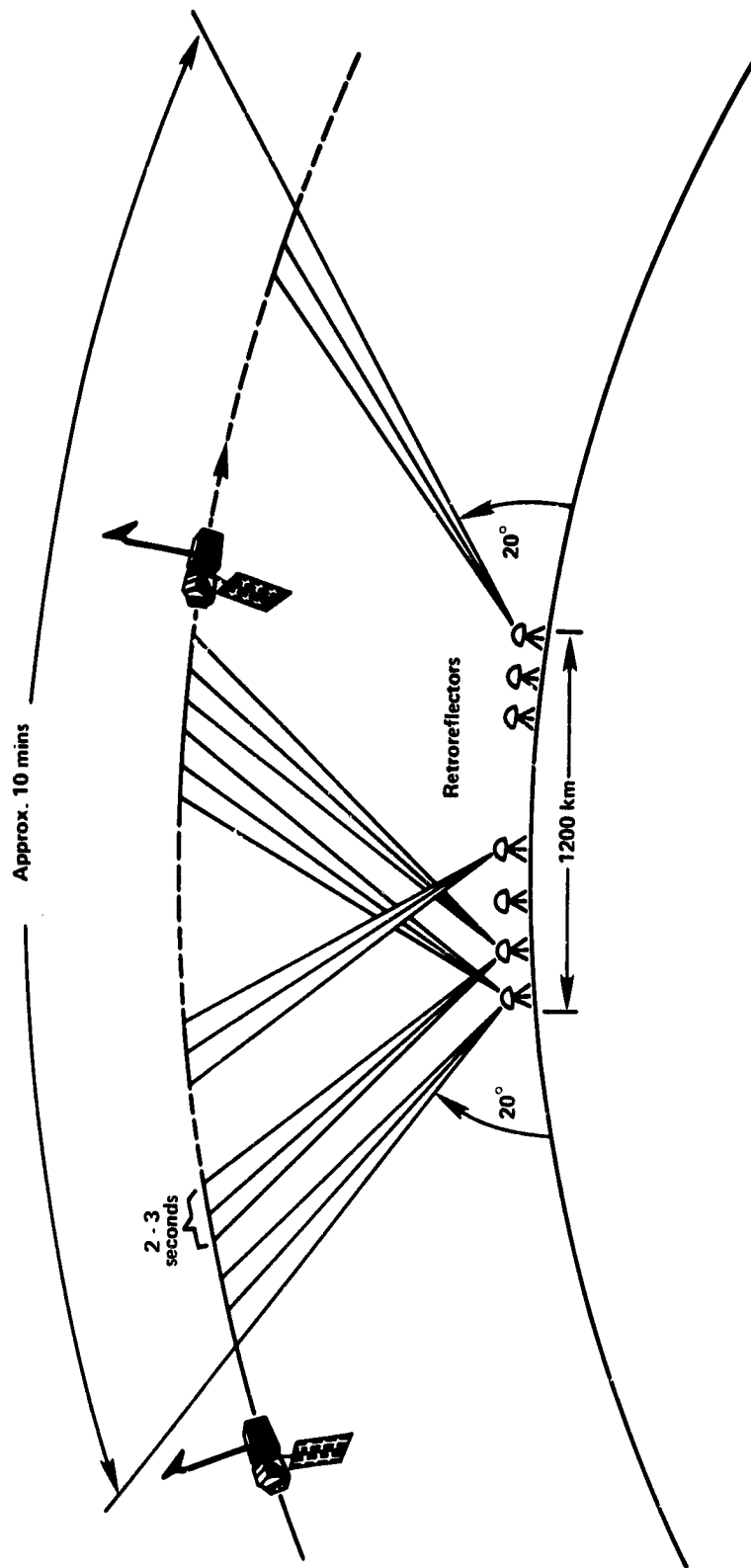


Figure 2. Sequence of Events as Spacecraft Passes Over a Network.

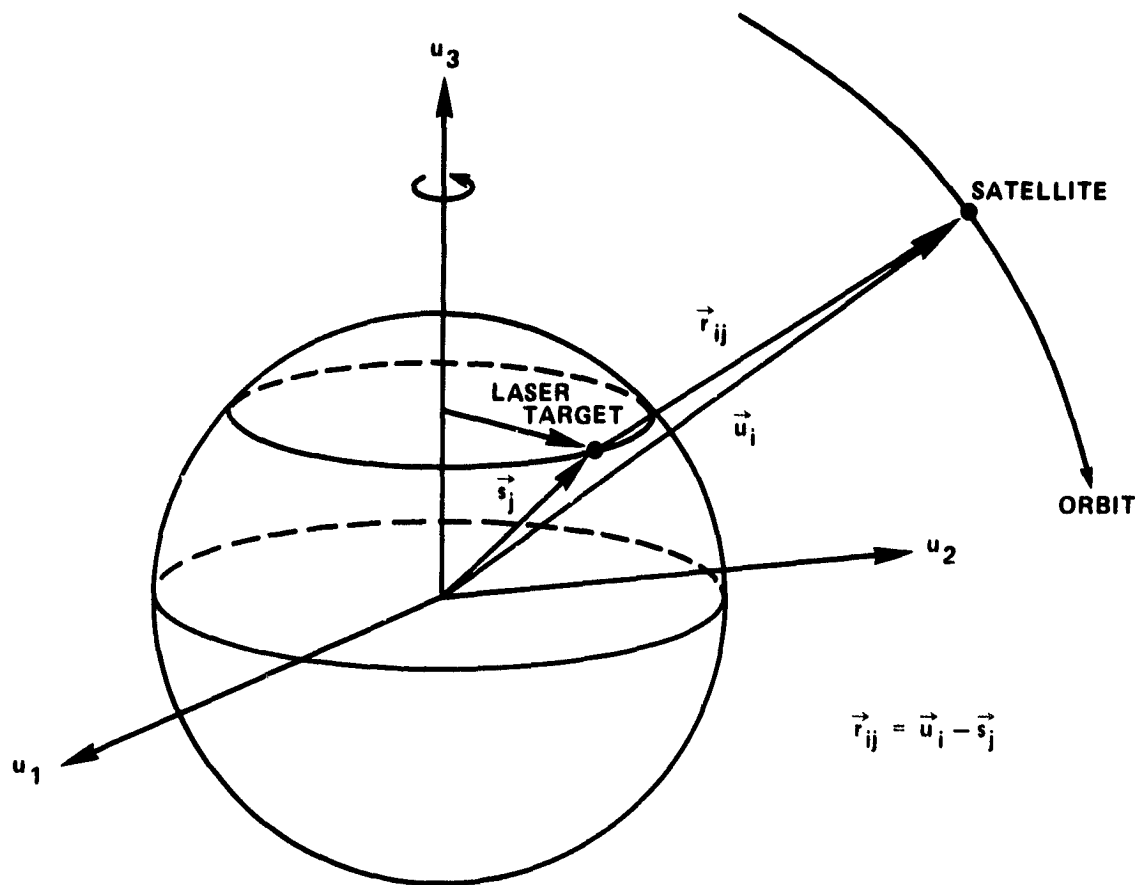


Figure 3. Spaceborne Laser Ranging System Measurement Geometry

Arrange all observations into a column vector

$$\vec{r} = \begin{bmatrix} r_1 \\ r_2 \\ \vdots \\ r_n \end{bmatrix} \quad (3)$$

(nX1)

From Equations (1) and (2)  $\vec{r}$  can be modelled by the non-linear equation

$$\vec{r} = F(\mathbf{Z}, \mathbf{L}) + \epsilon \quad (4)$$

The vector  $\mathbf{Z}$  contains epoch values of the parameters to be estimated (e.g. satellite state, reflector positions, etc.), and vector  $\mathbf{L}$  contains values of the unadjusted parameters which are assumed to be known constants in solving the regression equations (e.g. gravity coefficients, measurement biases, refraction errors, etc.), and  $\epsilon$  is the zero mean measurement noise vector. It is assumed that the elements of  $\epsilon$  are statistically independent. The final errors in the adjusted parameters can be decomposed into a component due to measurement noise, an alias component due to errors in the unadjusted parameters, (eg. the bias in the range measurement) and a component due to the errors in the a priori orbital state.

The errors in the measurement represented by Equation 4 can be approximated by a first order Taylor series expansion about some current nominal parameter values of the vectors  $\mathbf{Z}'$  and  $\mathbf{L}'$ . Then to first order

$$\begin{aligned} \delta\vec{r} &= \vec{r} - F(\mathbf{Z}', \mathbf{L}') = \mathbf{A}(\mathbf{Z} - \mathbf{Z}') + \mathbf{B}(\mathbf{L} - \mathbf{L}') + \epsilon \\ &= \mathbf{A}\delta\mathbf{Z} + \mathbf{B}\delta\mathbf{L} + \epsilon \end{aligned}$$

where

$$\mathbf{A} \equiv \left[ \frac{\partial F(\mathbf{Z}, \mathbf{L})}{\partial \mathbf{Z}} \right]_{\substack{\mathbf{Z} = \mathbf{Z}' \\ \mathbf{L} = \mathbf{L}'}} \quad (5)$$

$$\mathbf{B} \equiv \left[ \frac{\partial F(\mathbf{Z}, \mathbf{L})}{\partial \mathbf{L}} \right]_{\substack{\mathbf{Z} = \mathbf{Z}' \\ \mathbf{L} = \mathbf{L}'}}$$

where  $\mathbf{Z}'$  and  $\mathbf{L}'$  are the nominal values.

**A** and **B** are the sensitivity matrices associated with the adjusted and unadjusted parameters.

Given an unbiased a priori estimate  $\mathbf{Z}_0$  with error covariance matrix  $\mathbf{W}_0$ , the weighted least squares iteration for estimating  $\mathbf{Z}$  is given by

$$\hat{\mathbf{Z}} = \mathbf{Z}' + \left[ \mathbf{A}^T \mathbf{W}^{-1} \mathbf{A} + \mathbf{W}_0^{-1} \right]^{-1} \left[ \mathbf{A}^T \mathbf{W}^{-1} \delta \mathbf{F} + \mathbf{W}_0^{-1} (\mathbf{Z}_0 - \mathbf{Z}') \right]$$

where (6)

$$\mathbf{W} \equiv \mathbf{E}(\epsilon \epsilon^T)$$

On the first iteration,  $\mathbf{Z}'$  is usually chosen to be  $\mathbf{Z}_0$  but on subsequent iterations,  $\mathbf{Z}' = \hat{\mathbf{Z}}$

The estimated vector  $\hat{\mathbf{Z}}$  is subject to deviations in the a priori estimate, measurements, and unadjusted parameters, that is

$$\mathbf{Z} = \hat{\mathbf{Z}} + \delta \hat{\mathbf{Z}}$$

where (7)

where

$$\delta \hat{\mathbf{Z}} = \delta \hat{\mathbf{Z}}_0 + \delta \hat{\mathbf{Z}}_\epsilon + \delta \hat{\mathbf{Z}}_L$$

$\delta \hat{\mathbf{Z}}_0$ : Error in  $\hat{\mathbf{Z}}$  due to deviation in a priori estimate

$\delta \hat{\mathbf{Z}}_\epsilon$ : Error in  $\hat{\mathbf{Z}}$  due to deviation in measurement

$\delta \hat{\mathbf{Z}}_L$ : Error in  $\hat{\mathbf{Z}}$  due to deviation in the unadjusted parameters

$$\delta \hat{\mathbf{Z}}_0 = \left[ \mathbf{A}^T \mathbf{W}^{-1} \mathbf{A} + \mathbf{W}_0^{-1} \right]^{-1} \mathbf{W}_0^{-1} \delta \mathbf{Z}_0$$

(8)

$$\delta \hat{\mathbf{Z}}_\epsilon = \left[ \mathbf{A}^T \mathbf{W}^{-1} \mathbf{A} + \mathbf{W}_0^{-1} \right]^{-1} (\mathbf{A}^T \mathbf{W}^{-1} \epsilon)$$

$$\delta \hat{\mathbf{Z}}_L = \left[ \mathbf{A}^T \mathbf{W}^{-1} \mathbf{A} + \mathbf{W}_0^{-1} \right]^{-1} (\mathbf{A}^T \mathbf{W}^{-1} \mathbf{B}) \delta \mathbf{L}$$

If it is assumed that  $\delta \mathbf{Z}_0$ ,  $\epsilon$  and  $\delta \mathbf{L}$  are uncorrelated, then the overall covariance matrix associated with the estimated parameter vector  $\hat{\mathbf{Z}}$  is

$$\begin{aligned} \mathbf{E}(\delta \hat{\mathbf{Z}} \delta \hat{\mathbf{Z}}^T) &= \left[ \mathbf{A}^T \mathbf{W}^{-1} \mathbf{A} + \mathbf{W}_0^{-1} \right]^{-1} \\ &+ \left[ \mathbf{A}^T \mathbf{W}^{-1} \mathbf{A} + \mathbf{W}_0^{-1} \right]^{-1} (\mathbf{A}^T \mathbf{W}^{-1} \mathbf{B}) \mathbf{W}_L (\mathbf{B}^T \mathbf{W}^{-1} \mathbf{A}) \left[ \mathbf{A}^T \mathbf{W}^{-1} \mathbf{A} + \mathbf{W}_0^{-1} \right]^{-1} \end{aligned}$$

(9)

where

$$\mathbf{W}_L \equiv \mathbf{E}(\delta \mathbf{L} \delta \mathbf{L}^T)$$

In Equation 4 the parameter vector  $Z$  is represented by  $6m$  epoch states and  $3\ell$  laser target positions, that is

$$Z \equiv \begin{bmatrix} X_1 \\ X_2 \\ \vdots \\ X_m \\ S_1 \\ S_2 \\ \vdots \\ S_\ell \end{bmatrix} \quad (6m + 3\ell) \times 1 \quad (10)$$

Of interest are the relative positions of the laser targets with respect to each other. A convenient way of expressing this is in a tangent plane baseline coordinate system. This is obtained by differencing the station coordinates with respect to a master station

$$D = QZ \quad (11)$$

where  $D$  is the matrix consisting of all the intersite vectors related to a master station (target) and  $Q$  is a transformation matrix.

For example, for  $\ell$  laser targets with target number one being the master station and  $m$  satellite states

$$Q \equiv \begin{bmatrix} \underline{0} & \underline{I} & \underline{-I} & \underline{0} & \dots & \underline{0} \\ \underline{0} & \underline{I} & \underline{0} & \underline{-I} & \dots & \underline{0} \\ \vdots & \vdots & \vdots & \vdots & \dots & \vdots \\ \underline{0} & \underline{I} & \underline{0} & \underline{0} & \dots & \underline{-I} \end{bmatrix} \quad (3\ell - 3) \times (6m + 3\ell)$$

where

$$\begin{aligned} \underline{I} &\equiv \text{Identity matrix} \\ \underline{0} &\equiv \text{Null matrix} \end{aligned}$$

This differencing is followed by a rotation so that the errors are expressed as an along baseline component (in the tangent plane), a cross baseline component, and a vertical component.

$$\bar{D} = RD = RQZ \quad (12)$$

where

$$R \equiv \begin{array}{c|c|c|c} \mathbf{R}_1 & \mathbf{O} & \dots & \mathbf{O} \\ \mathbf{O} & \mathbf{R}_2 & \dots & \mathbf{O} \\ \vdots & \vdots & \dots & \vdots \\ \mathbf{O} & \mathbf{O} & \dots & \mathbf{R}_q \end{array} \quad (3\ell - 3) \times (3\ell - 3)$$

For each baseline there is a different rotation matrix  $\mathbf{R}_q$ .

Thus the covariance matrix in baseline coordinates is

$$E(\delta \bar{\mathbf{D}} \delta \bar{\mathbf{D}}^T) \equiv \mathbf{R} \mathbf{Q} E(\delta \hat{\mathbf{Z}} \delta \hat{\mathbf{Z}}^T) \mathbf{Q}^T \mathbf{R}^T \quad (13)$$

where  $E(\delta \hat{\mathbf{Z}} \delta \hat{\mathbf{Z}}^T)$  is given by Eqn. (9).

The covariance matrix  $E(\delta \bar{\mathbf{D}} \delta \bar{\mathbf{D}}^T)$  gives a measure of the uncertainty of the intersite vector  $\bar{\mathbf{D}}$ .

The repeated measurement of  $\bar{\mathbf{D}}$  gives the measurement precision.

If  $\bar{\mathbf{D}}_1$  is the 1st determination of the baseline vector over the survey period  $T_S$  and  $\bar{\mathbf{D}}_2$  is the second determination of the same baseline vector after a period  $T_R$  (the resurvey period) then

$$(\bar{\mathbf{D}}_1 - \bar{\mathbf{D}}_2) = \mathbf{R} \mathbf{Q} (\mathbf{Z}_1 - \mathbf{Z}_2) \quad (14)$$

and

$$\delta(\bar{\mathbf{D}}_1 - \bar{\mathbf{D}}_2) = \mathbf{R} \mathbf{Q} (\delta \mathbf{Z}_1 - \delta \mathbf{Z}_2) \quad (15)$$

The aim here is to obtain the measure of precision on the baseline vector  $\mathbf{D}_1$  and  $\mathbf{D}_2$ , that is

$$E \left\{ \delta(\bar{\mathbf{D}}_1 - \bar{\mathbf{D}}_2) \delta(\bar{\mathbf{D}}_1 - \bar{\mathbf{D}}_2)^T \right\}.$$

Using Equation (15) together with (7) and (8) yields this measure, that is:

$$E \left\{ \delta(\bar{\mathbf{D}}_1 - \bar{\mathbf{D}}_2) \delta(\bar{\mathbf{D}}_1 - \bar{\mathbf{D}}_2)^T \right\} = E(\mathbf{N}_1 \mathbf{N}_1^T) + E(\mathbf{N}_2 \mathbf{N}_2^T) + (\mathbf{P}_1 - \mathbf{P}_2) E(\delta \mathbf{L} \delta \mathbf{L}^T) (\mathbf{P}_1 - \mathbf{P}_2)^T$$

where

$$E(\mathbf{N}_k \mathbf{N}_k^T) = \mathbf{R} \mathbf{Q} (\mathbf{A}^T \mathbf{W}^{-1} \mathbf{A} + \mathbf{W}_0^{-1})_k^{-1} \mathbf{Q}^T \mathbf{R}^T \quad (16)$$

$$\mathbf{P}_k = \mathbf{R} \mathbf{Q} (\mathbf{A}^T \mathbf{W}^{-1} \mathbf{A} + \mathbf{W}_0^{-1})_k^{-1} (\mathbf{A}^T \mathbf{W}^{-1} \mathbf{B})_k$$

$$k = 1, 2$$

Note that the precision of the baseline vector is in essence noise limited, since the sensitivity to the uncertainty in geopotential inherent in matrix  $\mathbf{P}_k$  is almost the same from one survey

period  $T_S$  to the next survey period. Only second order temporal effects (ie, drag, earth rotation, solar pressure, refraction...) still remain and influence the precision of the intersite vector determination.

The precision in the baseline component of  $(\bar{D}_1 - \bar{D}_2)$  is  $\sigma_H$ . The corresponding elongation error is given by

$$\sigma_{\epsilon_H} = \frac{\sigma_H}{|\bar{D}|} \quad (17)$$

where

$|\bar{D}| \equiv$  magnitude of vector  $\bar{D}$  on the baseline length.

Baselines are frequently resurveyed a number of times. The estimated intersite distances can be fitted to a linear regression line (10) of the form

$$d(t) = d_0 + \dot{d}t \quad (18)$$

The elongation rates  $\dot{d}$ , determined by least squares, have a variance  $\sigma_{\dot{d}}^2$  which can be deduced from the least squares solution of Equation 18. That is

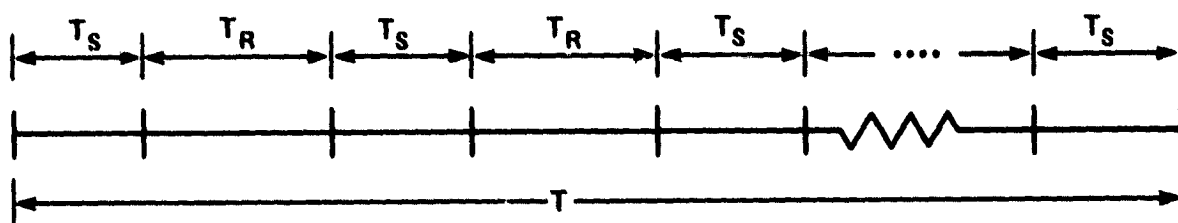
$$\sigma_{\dot{d}}^2 = \frac{n\sigma_d^2}{n\sum_{i=1}^n t_i^2 - (\sum_{i=1}^n t_i)^2} \quad (19)$$

where  $n$  is the number of measurements of the intersite distance of line  $d(t)$  and  $\sigma_d^2$  is the variance of  $d$ . If the measurements are made over time intervals  $T_S$  and repeated  $T_R$  time intervals apart, then at the end of  $T$  (days, weeks, . . .) (See Figure 4)

$$\sigma_{\dot{d}}^2 = \frac{12\sigma_d^2}{T^2} \left[ \frac{\frac{T}{T_S} \left( 1 + \frac{T_R}{T_S} \right)}{\left( 1 + \frac{T}{T_S} + \frac{T_R}{T_S} \right) \left( 2 + \frac{T}{T_S} + 2 \frac{T_R}{T_S} \right)} \right] \quad (20)$$

where

$T_S \equiv$  Survey period  
 $T_R \equiv$  Resurvey period  
 $T \equiv$  Total measurement period,



$T_S$ : Survey Period  
 $T_R$ : Resurvey Period  
 $T$ : Total Experiment Period

Figure 4. Relationship Between Survey, Resurvey and Total Experiment Periods.

From this, the elongation rate error  $\sigma_{\dot{\epsilon}_H}$  for a given baseline can be deduced. From Equation (17) and (20) one obtains

$$\sigma_{\dot{\epsilon}_H}^2 = \frac{12\sigma_{\epsilon_H}^2}{T^2} \left[ \frac{\frac{T}{T_S} \left( 1 + \frac{T_R}{T_S} \right)}{\left( 1 + \frac{T}{T_S} + \frac{T_R}{T_S} \right) \left( 2 + \frac{T}{T_S} + 2 \frac{T_R}{T_S} \right)} \right] \quad (21)$$

#### IV. SIMULATION RESULTS

A series of simulations have been performed of a survey of the States of California using a Spaceborne Laser Ranging System. In the simulations approximately 150 laser targets are distributed over California at a separation of 50 km (See Fig 5). The simulations estimate the precision with which the baseline distance can be obtained in the presence of noise and bias of the laser system; perturbations of the spacecraft motion and errors in the refraction calculations.

The orbit of the satellite is assumed to be circular at 1000 km and 50 degree inclination. A medium inclination orbit was chosen because it provides ground tracks across California in almost orthogonal directions (southwest to northeast and northwest to southeast) as shown in Fig. 6. This distribution of satellite ground tracks provides a strong geometric distribution of range measurements. In contrast, a polar orbit provides only north to south and south to north tracks and these provide strong geodetic ties in the north-south direction but only weak control in the east-west direction.

The simulations have been conducted over survey intervals ( $T_S$ ) of 1, 3, and 6 days respectively assuming 50% cloud cover that for the six day observation period reduces the number of successfully observed tracks over the area from 36 to 18. For all the simulations the data on the observed tracks is assumed to be taken at the rate of 10 pulses per second with a noise of 2 cm and a bias of 0.3 cm. The effect of errors in the gravity field on the motion of the satellite were accounted for by adopting the GEM-10 covariance model of the gravity field derived from satellite tracking and surface gravity data (11). The effects of solar radiation pressure and air drag on the satellite were

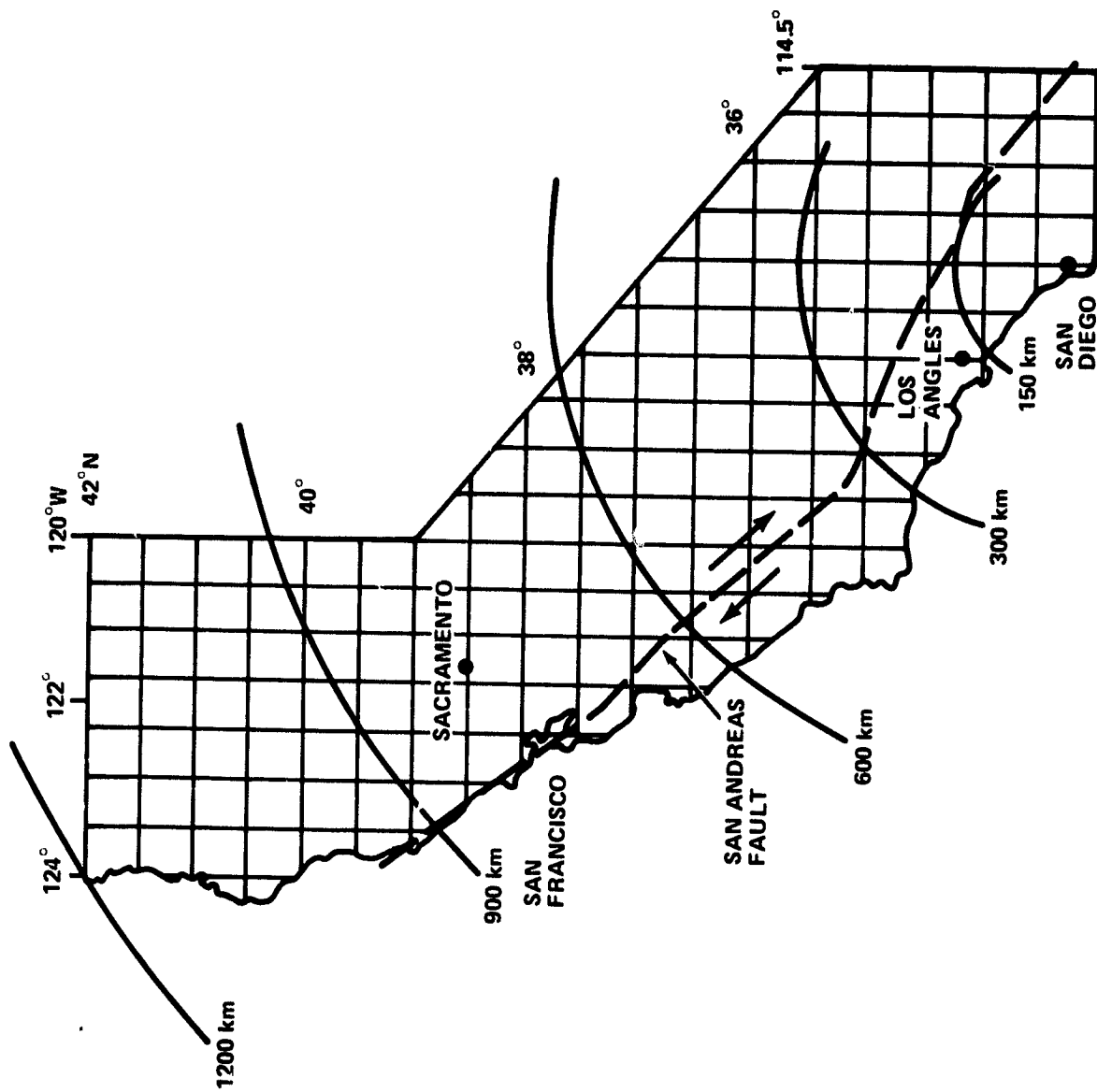


Figure 5. Distribution of Ground Targets for California Simulation (Spacing Approx. 50 km)

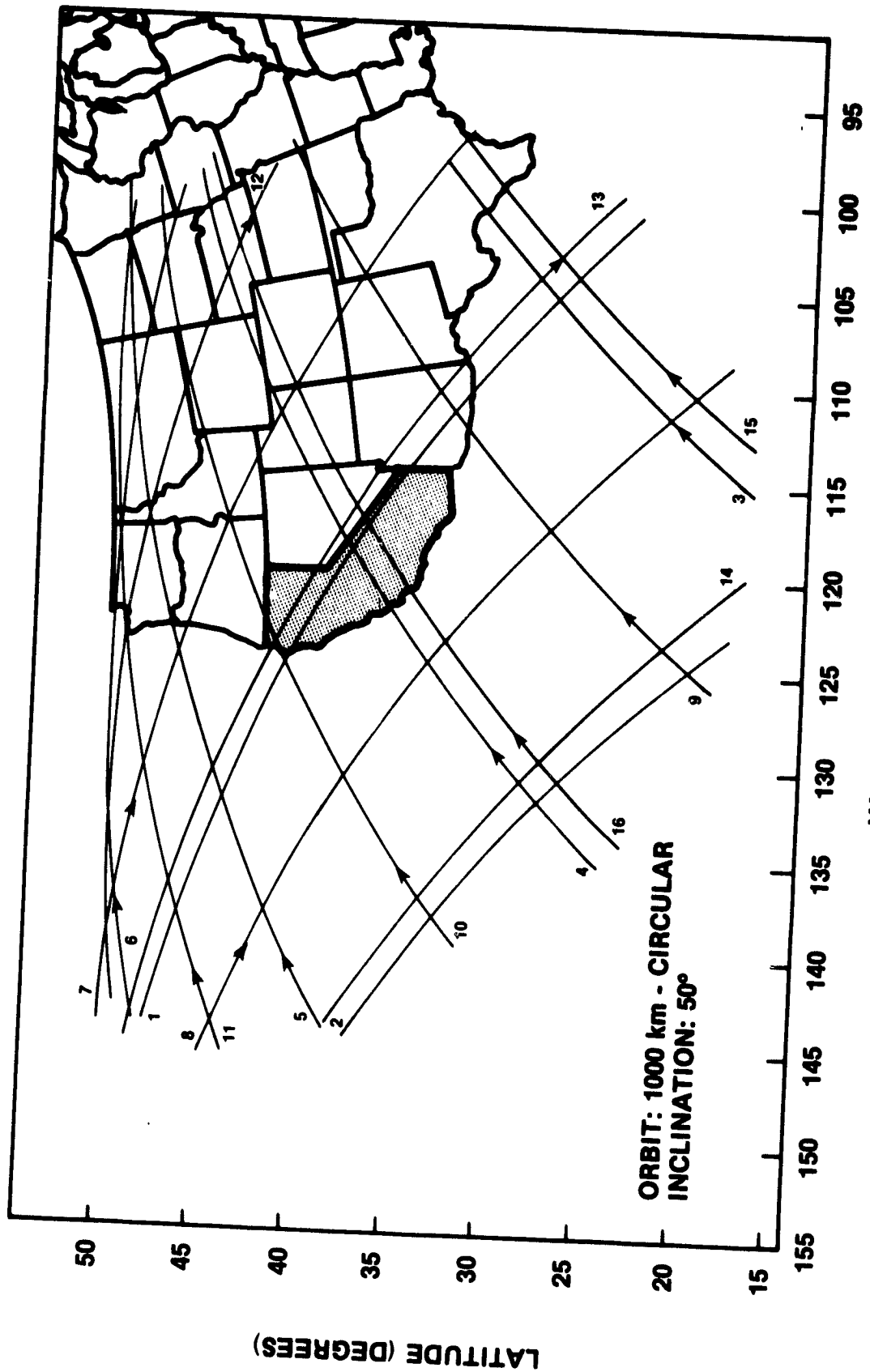


Figure 6. Ground Tracks - Spaceborne Ranging System

assumed to be in error by a constant percentage in their estimation of their effect on the solutions. Based on operational experience, the radiation pressure error is assumed to be 30% of the nominal and the atmospheric drag 20% of the nominal. The effect of atmospheric refraction errors were estimated through a two parameter (ie pressure and PTK gradient) model (12). In this model, the temperature and pressure are assumed known at a limited number of locations in the region and are used to develop an atmospheric model of the whole region from which the temperature, pressure and PTK gradients at each of the laser targets can be estimated. The pressure error of  $\pm 1.0$  mbar chosen for the error analysis represents a realistic estimate for the pressure measurement accuracy at weather stations. Walter Hoehne specified in (13) accuracy figures of  $\pm 0.2$  mb for a mercury barometer and  $\pm 0.5$  mb for an aneroid barometer. Either of these instruments may be used at a weather station. In addition, an analysis of meteorological data from 48 weather stations in Southern California and Nevada (12) has shown that the pressure measurement residuals from a regression fit vary from  $\pm 0.4$  mb to  $\pm 0.9$  mb.

Figure 7 shows the baseline precision as a function of the baseline length. This measure of precision for a 50 km baseline is about 0.3 cm and increases to 1 cm for a 1200 km baseline. For baseline lengths up to 300 km, the precision is primarily dependent on system noise, but for longer baselines, say from 400 km to 1200 km, the uncertainty in the geopotential becomes the dominant error source. For a system noise of 3 cm, the noise curve in Fig 7. will be shifted upward by a factor of 1.5 for baselines less than 400 km and then the unadjusted parameters, predominantly the uncertainty in the Earth's gravity field, dominate the precision for longer baselines.

Figure 8 shows the improvement in the precision in the measurement of baseline distances which results for increasing the survey period  $T_S$ . An increase in the survey period from 3 to 6 days results in only a small improvement in the baseline precision.

From the knowledge of the precision with which baseline determinations can be made, the elongation rate precision can be calculated from Equation 21.

Fig 9. shows the elongation rate precision for a 50 km baseline as a function of the measurement program period  $T$ . For the calculation of elongation rate precision, a survey period  $T_S$  of six days

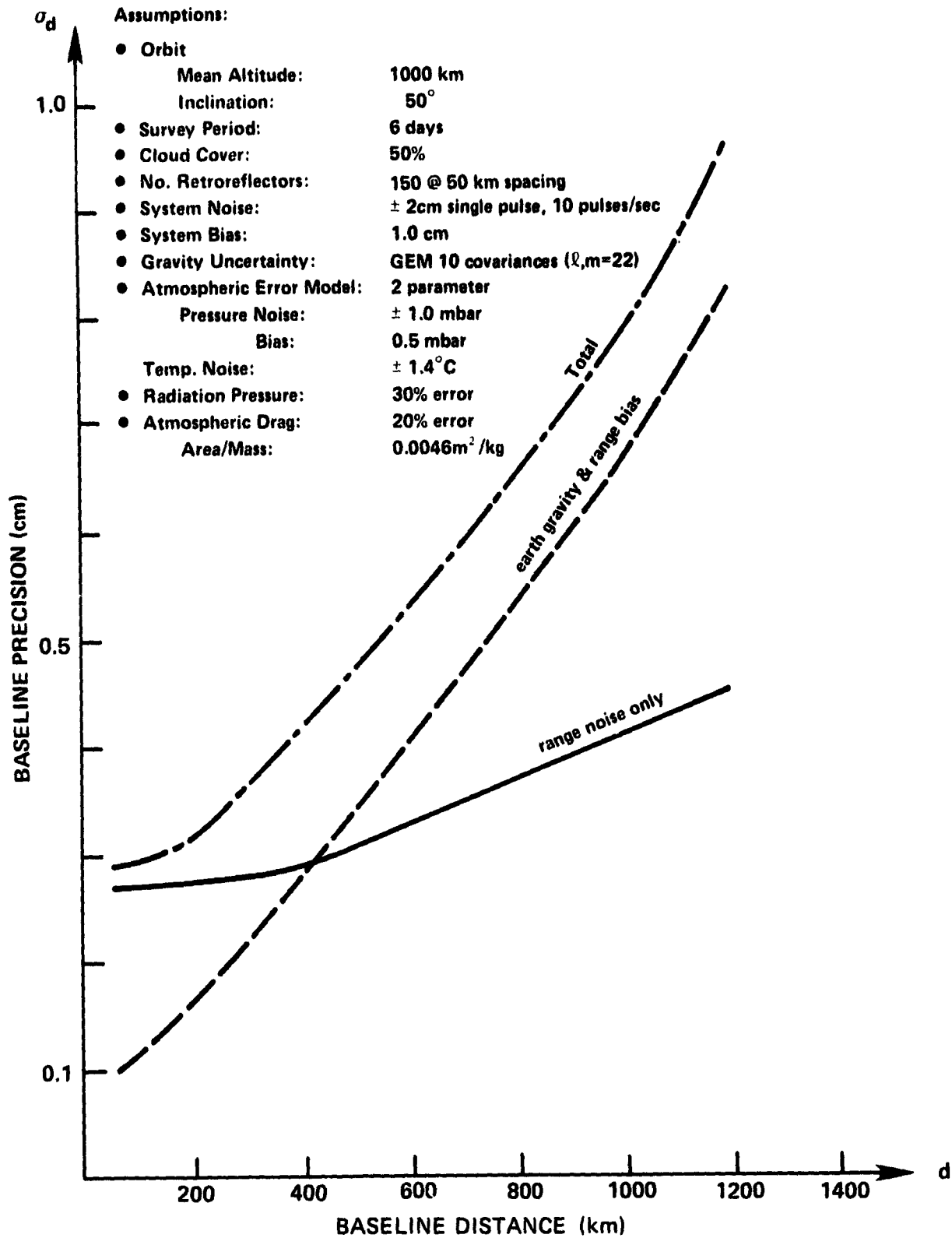


Figure 7. Baseline Precision vs Baseline Distance

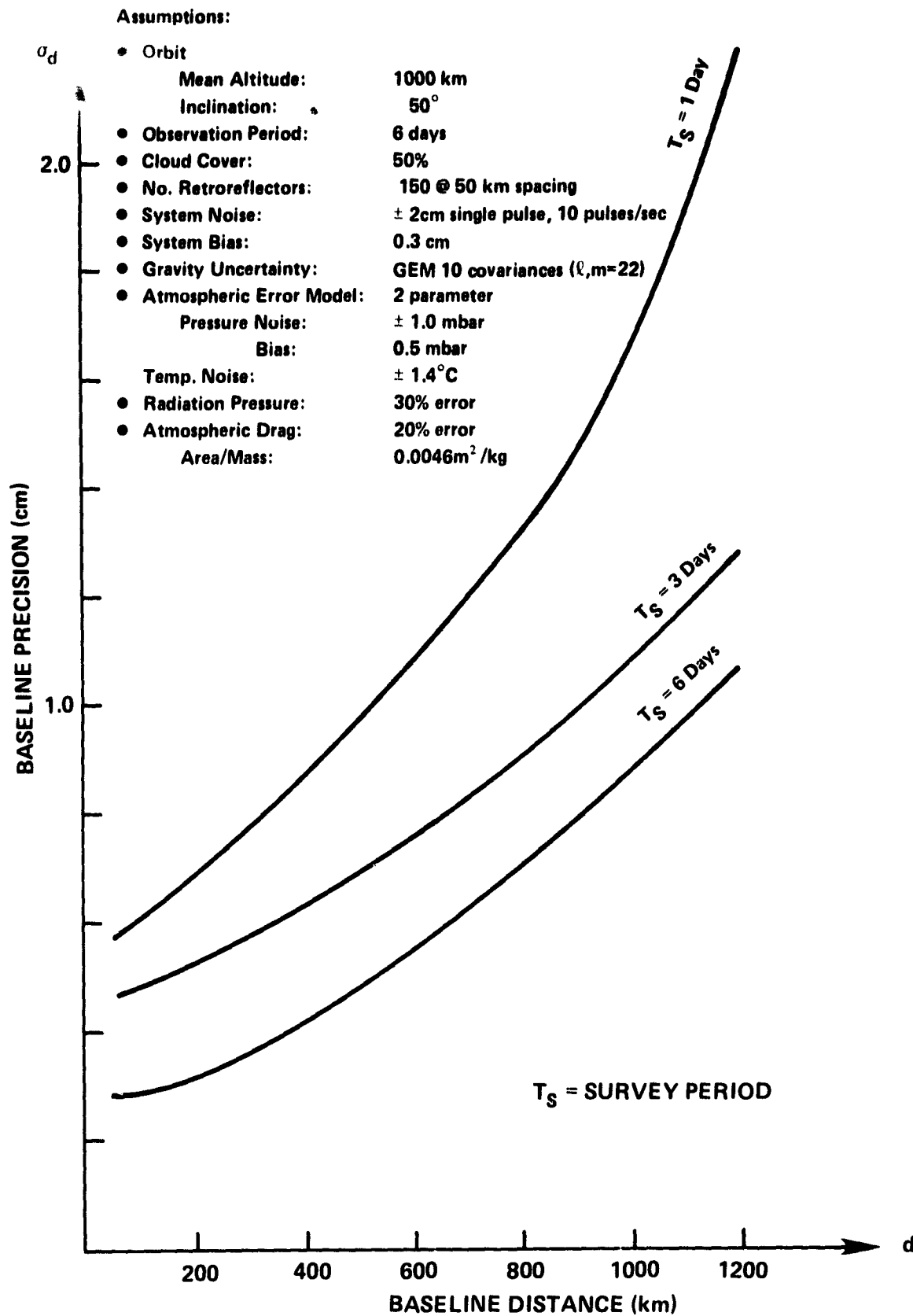


Figure 8. Baseline Precision vs Baseline Length

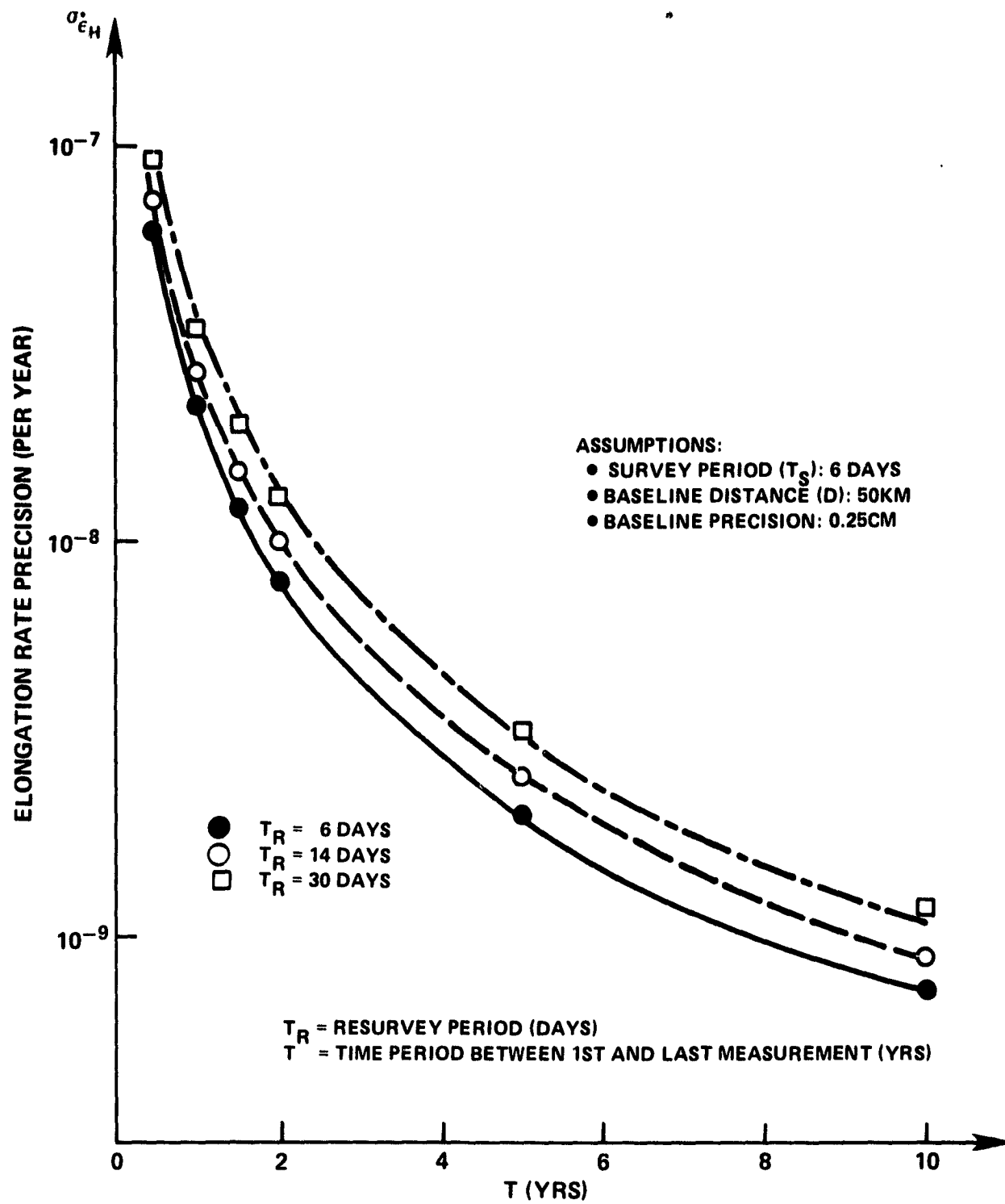


Figure 9. Elongation Rate Precision vs Total Measurement Periods.

was assumed and an interval between surveys, the resurvey period,  $T_R$ , of 6, 14, and 30 days was chosen. As can be seen from this figure, the Spaceborne Laser Ranging System has the capability of determining elongation rates to a precision of better than  $1 \times 10^{-8}$  strain per year over a 2½ to 3 year period T. Furthermore, an order of magnitude improvement in the elongation rate precision can be achieved over a five year period by making continuous measurements over about a week every other month. The figure also shows that little improvement in the elongation rate determinations is achieved by increasing the measurement frequency (ie decreasing the resurvey period  $T_R$ ). This means power for the laser system can be conserved and thus the system's lifetime extended without degrading the measurement precision. Finally, Figure 9 shows that elongation rate measurements to better than  $1 \times 10^{-9}$  per year may be possible within a decade or less of measurements.

## V. CONCLUSION

It is shown that the concept of a Spaceborne Laser Ranging System has the capability to (a) determine baselines to a precision of less than 1 cm over distances of up to 1000 km; and (b) determine the elongation rate to a precision of better than 1 part in  $10^8$  per year during a period of 2 yrs. Such a system could provide a capability to observe the precursory geodetic motions believed to occur before large earthquakes. Indeed, established on a global scale, with survey areas around all major seismic zones, the Spaceborne Laser Ranging System could provide the first real probability for "capturing" a magnitude 7.5, and above, earthquake.

In addition, general geodetic survey work can be performed accurately and very rapidly with minimal incumbrance by the terrain.

## VI. ACKNOWLEDGMENTS

The authors are indebted to Dr. M. W. Fitzmaurice and Messrs. P. O. Minott and D. Premo who have played a major part in developing the concept of the Spaceborne Laser Ranging System.

## REFERENCES

1. Vonbun, F. O., Kahn, W. D., Argentiero, P. D., and Koch, D. W. "Spaceborne Earth Applications Ranging System (SPEAR)." *Journal of Spacecraft and Rockets*, Vol 14, No. 8, August 1977, pp. 492-495.
2. Smith, D. E. "Spaceborne Ranging System." *Proceedings of the Ninth Geodesy/Solid Earth and Ocean Physics (GEOP) Research Conference*. Oct. 2-5, 1978; Department of Geodetic Science Report No. 280, The Ohio State University, pp. 59-64.
3. Smith, D. E., Tapley, B. D. "The Report From The Workshop On the Spaceborne Geodynamics Ranging System." IASOM TK 79-2 Institute for Advanced Study In Orbital Mechanics, The University of Texas at Austin, Austin, Texas, March 1979.
4. Mueller, I. I., Van Gelder, B. H. W., Kumar, M. "Error Analysis For The Proposed Close Grid Geodynamic Satellite Measurement System (CLOGEOS)." Department of Geodetic Science Report No. 230, The Ohio State University, Sept. 1975.
5. Fitzmaurice, M. W. "NASA Ground Based and Space-Based Laser Systems." NASA Technical Report 1149, January 1978.
6. Berger, J. (Private Communication) Institute of Geophysics And Planetary Physics, University of California at San Diego.
7. Anderson, D. L. (Private Communication) Seismological Laboratory, California Institute of Technology, Pasadena, CA.
8. Fitzmaurice, M. W. (Private Communication) Goddard Space Flight Center, Greenbelt, MD.
9. Minott, P. O. (Private Communication) Goddard Space Flight Center, Greenbelt, MD.
10. Cohen, S. C., Cook, G. R., "Determining Crustal Strain Rates with a Spaceborne Geodynamics Ranging System Data; *Manuscripta Geodetica*, Vol. 4 (1979) pp. 245-260.

11. Leach, F. J., Klosko, S. N., Laubscher, R. E., Wagner, C. A. "Gravity Model Improvement Using GOES-3 (GEM 9 and 10). GSFC X-921-77-246, Sept. 1977.
12. Gardner, C. S. "Comparison Between Refraction Covariance Model and Ray Tracing." Radio Research Laboratory Publication No. 486, College of Engineering, University of Illinois, Urbana, Illinois, 1977.
13. Hoehne, W. "Standard No. D 3631-77." 1978 ASTN Book of Standards Vol. 26.
14. Gibbs, B. P. "Evaluation of Polynomial Regressions For Pressure And Temperature Data." BTS Report TR-78-53, Feb 1978.